Desalination and Water Treatment
www.deswater.com

doi:10.5004/dwt.2017.21712

98 (2017) 85–91
December

Sensitivity analysis of parameters on pure water flux for inside-out hollow ultrafiltration membrane fiber

Yanning Wang[a,b], Hongying Yuan[a,b,*], Zhichao Zhang[a,b], Yuzhong Zhang[c,d], Dawei Jing[a,b]

[a]*School of Environmental and Municipal Engineering, Tianjin Chengjian University, Tianjin, China, Tel. +8622-23085117, email: wangyanning@tcu.edu.cn (Y.N. Wang), zhangzhichao609@163.com (Z.C. Zhang), david_j5996@163.com (D.W. Jing)*
[b]*Tianjin Key Laboratory of Aquatic Science and Technology, Tianjin 300384, China, Tel. +86-22-23085117, email: yuanhy_00@163.com (H.Y. Yuan)*
[c]*School of Materials Engineering, Tianjin Polytechnic University, Tianjin, China, email: zhangyz2004cn@vip.163.com (Y.Z. Zhang)*
[d]*State Key Laboratory of Separation Membranes and Membrane Processes, Tianjin 300387, China*

Received 5 June 2017; Accepted 21 November 2017

ABSTRACT

The internal factors that affect the flux of inside-out hollow UF (ultra filtration) membrane fiber were simplified as "fiber radial permeability coefficient" and "fiber axial resistance coefficient". The two coefficients were tested and analyzed by using hydrophilic short fiber and hydrophobic fiber respectively. A filtration mathematical model was successfully developed to describe the operation of the hollow fiber. The sensitivity function of average pure water flux, such as fiber length, inside diameter and permeability coefficient, was established. The influence of single parameter change on pure water flux of membrane fiber was analyzed. The results showed that the longer the film length was, the lower the average flux was; the bigger the wire diameter was, the higher the average flux was; the higher the temperature was, the greater the average flux was; the higher the pressure was, the greater the average flux was.

Keywords: Hollow ultrafiltration; Inside-out hollow fiber; Pure water average flux; Sensitivity analysis

1. Introduction

With ultra filtration technology being used more and more widely in such fields as municipal engineering and industrial water treatment [1–3], requirements for membrane properties are increasingly high. The product-water flux of ultra filtration membrane fiber serves as a critical index in the test of membrane properties.

In-depth research has been conducted by many scholars on membrane flux. Li et al. [4] put forward the concept of zero pollution flux, suggesting that under this condition, the irreversible membrane pollution is extremely slight or even none at all. Li et al. [5–7] established the mathematical model of hydromechanics based on hollow fiber membrane filtration, explaining the pattern of how operation flux and the configuration of fiber membranes influence partial filtration, that is, the uniformity of point flux distribution increases along with the increase in fiber membrane length, operation flux and the intrinsic resistance of membrane and the decrease in the inner diameter of the fiber membrane. Zhuang et al. [8,9] set up a 3-D porous media model for hollow fiber ultra filtration membrane components, by which the 3-D distribution of component flux was obtained and the impacts of the pressure difference between the inlet and the outlet as well as the water permeability on flux distribution were studied. Based on their research, the flux distribution of any film and membrane bundle is heterogeneous in three-dimensional space, with partial high flux adding to energy-consumption of the equipment and reducing the efficiency of components. Both the increase of the pressure difference between the inlet and the outlet and the water

*Corresponding author.

permeability will lead to the decrease in the homogeneity of flux distribution. Liu, Lv et al. [10] thought that the guiding role of critical operation flux has more significance in actual application in engineering. Zhang et al. [11] established a mathematical model of the uncertainty analysis for pure water flux measurement, finding that uncertainty derives from repeated measurements of water temperature. By finite element numerical simulation, Gunther et al. [12] studied how the filling density under pure water conditions affects the flux distribution along lengthwise direction: when the filing density is relatively large, the flux at the bottom of the membrane fiber is larger; otherwise the flux at the top of the membrane fiber is larger. Polyakov [13] developed a mathematical model to describe the performance of dead-end outside-in hollow fiber filters. Lin [14], Pavanasam [15] and Alventosa-Delara [16] established two polynomial regression model to study the influence of different factors on interception ratio. Yoon, Lee, Yeom [17] demonstrated a news experimental method to obtain internal pressure profiles in a hollow fiber membrane. It indicated that the local flux near membrane exit was lower than those in adjacent area. Lim et al. [18] studied several design feature of hollow fiber membrane modules to analyse the corresponding changes to the local flux distribution and permeate output flow rate using CFD. Mehdipourghazi et al. [19] developed a 2D mathematical model with axial and radial diffusions in the membrane contractor.

Most of the researches above take membrane components as the research object and analyzes flux distribution features from a macro point of view. This paper is oriented at single membrane fibers, discussing the sensitivity function between parameters such as fiber length, temperature, pressure, fiber diameter and pure water flux [20], and analyzing the influence of the increment of each parameter on pure water flux.

An important technical parameter reflecting the performance of inside-out hollow fiber UF membrane is the average pure water flux of membrane fibers under standard testing conditions (“pure water flux” in short). Here the standard testing conditions mainly include three aspects: single-ended water production, feed water temperature of 25°C, and transmembrane pressure difference of 0.1 MPa.

As ultra filtration membrane fiber is a pressure-driven membrane process and a hollow fiber structure, its main performance indexes include “fiber wall permeability coefficient” and “lengthwise resistance coefficient”. In terms of hollow ultra filtration membrane fiber, it varies not only in specifications of fiber length and diameter, but also in membrane materials, structures, processes, aperture, porosity and fiber wall thickness, etc. Thus there is great difference in the “fiber wall permeability coefficient” which represents the permeability performance of membrane fibers of different types. Therefore, pure water flux, which serves as an indicator of the overall performance of membrane fibers, will vary with different parameters such as fiber length, diameter and wall permeability coefficient.

If the actual measurement of different membrane fiber parameters is adopted to determine the relation between various parameters and pure water flux, the workload will be heavy and effective conclusion will be unavailable due to the interference of tests errors [21]. Hence a mathematical operation model of inside-out hollow fiber UF membrane can be established based on measurement results of the fiber radial permeability coefficient and the fiber axial resistance coefficient in order to obtain the sensitivity function between the increment of such parameters as fiber length, fiber diameter and permeability coefficient and pure water flux, that is, to analyze the degree of influence of various parameter increments on pure water flux in a relatively strict way. The special performance of membrane fiber can thus be effectively reflected or predicted, and related preparations effectively guided.

2. Testing equipment and characteristic coefficients

In this paper, the test membrane fiber has the following specifications: Polyether sulfone (PES) , inner diameter of 0.8 mm, outer diameter of 1.4 mm, its molecular weight cut-off 65000 Da, the porosity 85%, and manufacturer: Tianjin University of Technology, China.

The test device is shown in Fig. 1. The water temperature is controlled by a thermostat, the working pressure is controlled by a pressure relief valve, and the pressure of the membrane fiber is measured with a pressure gauge. Fig. 1 (a) is a hydrophilic short fiber test. The length of the fiber is 0.1 m, which is used to measure the fiber radial permeability coefficient. The shorter length of the fiber can ensure a relatively constant pressure along the line. Fig. 1 (b) is a hydrophobic filament test. The wire length is 0.3 m, which is used to measure fiber axial resistance coefficient. The longer wire length can ensure a relatively constant flow rate. Hydrophilic membrane fiber can be used as hydrophobic membrane fiber after hydrophobic treatment.

In Fig. 1, the tested membrane fiber is placed horizontally, with zero pressure outside the fiber and no elevation pressure difference between the water on the two sides of the fiber. In actual engineering, the membrane fiber is placed upright, and the elevation pressure difference between the water on the two sides of the fiber is mutually offset, thus the testing method in the figure is able to reflect the actual operating mode. The height influence when the membrane fiber is operating upright is not taken into account in the tests and pressure data calculated in this paper. If the influence is considered, elevation pressure shall be added as the height increases. In addition, the following analyses ignore the impacts of temperature, pressure and hydrophobic treatment on fiber length and fiber diameter.

3. The two characteristic coefficients of inside-out hollow fiber

3.1. The fiber radial permeability coefficient of hydrophilic short fiber

When conducting a performance test on single inside-out hollow fiber, there is a large space outside the fiber in which the flow rate is very low, so zero constant pressure can be presumed. The compact layer is at the inner side of the fiber, so the permeability area is calculated based on the inner diameter *d*. Therefore, according to the mathematical model of pressure-driven membrane processes, the product water flow rate $\Delta\theta_s$ of short hydrophilic fiber can be expressed as follows:

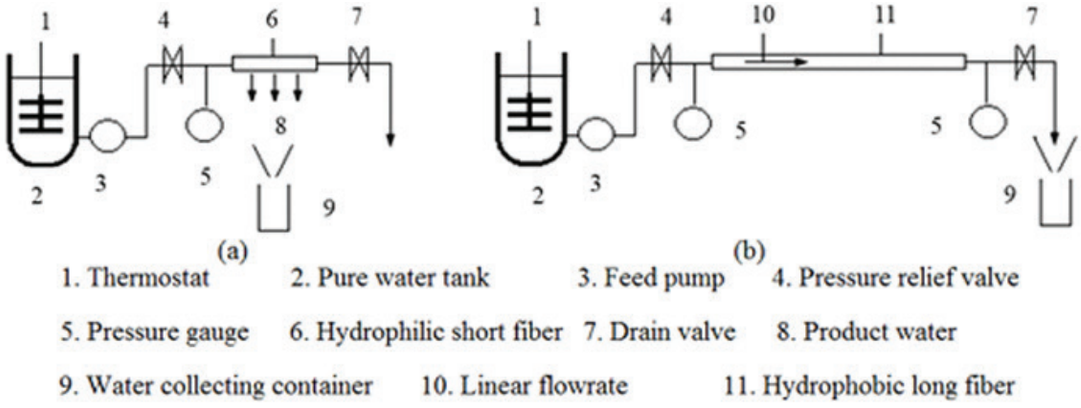

Fig. 1. Testing equipment for characteristic coefficients of inside-out hollow fiber (a) Test equipment for the fiber radial permeability coefficient of hydrophilic short fiber; (b) Test equipment for the fiber axial resistance coefficient of the hydrophobic long fiber.

$$\Delta\theta_s = A \cdot S \cdot (p-0) = A(T,p) \cdot \pi \cdot d \cdot \Delta l_s \cdot (p-0) \tag{1}$$

In which S represents the inner wall area of the short membrane fiber, ΔL_s is the length, d is the inner diameter, T is the feed water temperature, p is the feed water pressure, zero is the outside pressure of the membrane fiber, $A(T,p)$ is the fiber radial permeability coefficient which is related to the temperature T and the pressure p.

In regard of the temperature T and the pressure p in Eq. (1), an orthogonal test for hydrophilic short fiber is conducted by way of two variables & five levels. The tests results are processed in numerical fitting, before obtaining a polynomial of power functions indicating the features of the temperature T and Pressure p of fiber radial permeability coefficient A:

$$A(T,p(l)) = -5.34\times10^{-10} + 9.34\times10^{-11}\times T + 1.47\times10^{-15}\times p(l) + 3.17\times10^{-17} \times T\times p(l) - 1.58\times10^{-12}\times T^2 - 4.72\times10^{-21}\times p(l)^2 \tag{2}$$

In the equation above, the inner pressure p is presented as $p(l)$, a function of flow location l, in order to prepare for the following calculation of the membrane fiber operation model.

3.2. The fiber axial resistance coefficient of the hydrophobic long fiber

According to the theory of hydrodynamics, in circular tube flow channels, if the flow rate is lower than the critical Reynolds number, the relation between the on-way pressure drop and the flow rate can be explained by a linear equation; while if the flow rate is higher than the critical Reynolds number, the relation can be explained by a quadratic equation. Results of tests conducted on hydrophobic long fibers have proved that although the inner flow rate is lower than the critical Reynolds number, the relation between the on-way pressure drop Δp_l is related to both the runoff speed in first and second power as the membrane fiber is not a standard round tube, the fiber diameter is not in uniformity, and the materials are not rigid.

$$\Delta p_l(l) = \mu(T) \cdot \frac{128 \cdot \Delta l_l}{\pi \cdot d^4}(e_1 \cdot q(l) + e_2 \cdot q(l)^2) \tag{3}$$

In the equation above, $\mu(T) = (1.72 - 0.0457T + 0.0005T^2) \times 10^{-3}$ indicates the water viscosity coefficient related to the specific temperature, q refers to the inner on-way flow rate, ΔL_l the length of the membrane fiber and $e_1 e_2$ the correlation coefficients between the on-way pressure drop and the on-way flux.

In the regard of flow rate q in Eq. (3), a test for hydrophobic long fiber is conducted via a five-level method and the test results are processed in numerical fitting in order to obtain $e_1$and e_2 in the friction drag coefficient $E = (e_{1,} e_2)$:

$$e_1 = 0.60; \quad e_2 = 1.39 \times 10^6 \tag{4}$$

4. The mathematical operation model of inside-out hollow fiber

The mathematical operation model of inside-out hollow fiber is based on the membrane fiber structure and its differential parameter as is shown in Fig. 2. In which, d represents the inner diameter of the membrane fiber, L the fiber length, l the location, p (l) the on-way pressure at point l, q (l) the on-way flow rate at point l, $\Delta\theta$ (l) the water yield flux within the length of Δl and P_0 is the feed water pressure.

In accordance with pressure-driven ultra filtration membrane process relations, the produced water flow rate $\Delta\theta$ (l) within the length of Δl can be expressed as follows:

$$q(l) - q(l+\Delta l) = \Delta\theta(l) = A(T,p(l)) \cdot \pi \cdot d \cdot \Delta l \cdot p(l) \tag{5}$$

In the equation above, A (T, $p(l)$) is the fiber radial permeability coefficient related to the specific temperature T and the pressure p (l).

Based on the relation between Eqs. (2) and (5), the mathematical operation model of inside-out hollow fiber under a trans membrane pressure difference of 0.1*MP a* can be explained with the following differential equation:

$$\begin{cases} \dfrac{dq(l)}{dl} = \lim\limits_{\Delta l\to 0}\dfrac{q(l+\Delta l)-q(l)}{\Delta l} = \lim\limits_{\Delta l\to 0}\dfrac{-\Delta\theta(l)}{\Delta l} = -A(T,p(l))\cdot\pi\cdot d\cdot p(l); \quad q(L)=0 \\ \dfrac{dp(l)}{dl} = \lim\limits_{\Delta l\to 0}\dfrac{p(l+\Delta l)-p(l)}{\Delta l} = -\mu(T)\dfrac{128}{\pi\cdot d^4}(e_1\cdot q(l)+e_2\cdot q(l)^2); \quad (p(L)+p(0))/2 = 0.1 \end{cases} \tag{6}$$

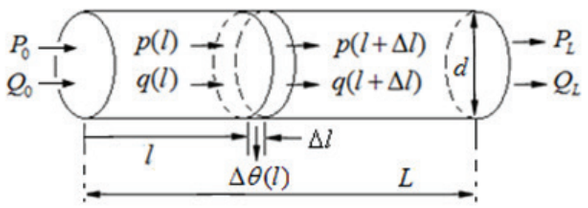

Fig. 2. The structure and differential parameter of inside-out hollow fiber.

For the membrane fiber structure shown in Fig. 2 and its differential parameter, the produced water flux δ(l) located at point l can be expressed as:

$$\delta(l) = A(T, p(l)) \cdot p(l) \tag{7}$$

Therefore, the pure water flux of the whole inside-out hollow fiber can be defined as:

$$F = \int_0^L \delta(l) dl / L \tag{8}$$

5. The sensitivity function of pure water flux to the increment in various parameters

In practice, different types of membrane fibers with different specifications have different pure water flux. Different specifications manifest in various fiber lengths and fiber diameters. Therefore, pure water flux F can be expressed as a function of the fiber length increment ΔL and the inter diameter increment Δd. Since the difference between fiber types is determined by the difference in produced water flux under the same feed water temperature and feed water pressure, pure water flux F can be expressed as a function of the temperature increment ΔT and the pressure increment ΔP. Here, the fiber length increment ΔL and the fiber inner diameter increment Δd are structural increments, while the temperature increment ΔT and the pressure increment ΔP only change the fiber radial permeability coefficient. Eq. (2) can thus be converted into:

$$\begin{aligned} &A(T+\Delta T, p(l)+\Delta P) = -5.34\times10^{-10} + 9.34\times10^{-11}\times(T+\Delta T) \\ &+1.47\times10^{-15}\times(p(l)-\Delta P) + 3.71\times10^{-17}\times(T+\Delta T)\times(p(l)+\Delta P) \\ &-1.58\times10^{-12}\times(T+\Delta T)^2 - 4.72\times10^{-21}\times(p(l)+\Delta P)^2 \end{aligned} \tag{9}$$

The standard parameters for defining "specific membrane fiber" are: fiber length L = 1.5 m, inner diameter d = 0.8 mm, temperature T = 25°C, operating pressure P = 100 kPa, namely ΔT = 0, ΔP = 0, ΔT = 0, ΔP = 0. When the value of ΔT is negative, the fiber radial permeability coefficient of the corresponding fiber is lower than that of the "specific membrane fiber", and the corresponding fiber can be called as "high-temperature membrane fiber". Otherwise, when ΔT is positive, the corresponding fiber can be called "low-temperature membrane fiber". Likewise, when ΔP is negative, the fiber radial permeability coefficient of the related fiber is lower than that of the "specific membrane fiber", so the related fiber can be called as "high-pressure membrane fiber". Otherwise, when ΔP is positive, the related fiber can be called "low-pressure membrane fiber". The physical feature of the high-temperature fiber or the high-pressure fiber is probably a smaller membrane aperture, a lower porosity or a poorer permeability of membrane materials. On the contrary, the physical feature of the low-temperature fiber or the low-pressure fiber might be a larger membrane aperture, a higher porosity or a better permeability of membrane materials.

In other words, if the pure water flux F of the "specific membrane fiber" is a_0, under standard testing conditions, the pure water flux sensitivity ΔF of "non-specific membrane fibers" shall be expressed as a function of various parameter increments: i.e. ΔF (ΔL, Δd, ΔT, ΔP). This function with four variables can be expressed as the following polynomial of power functions:

$$\begin{aligned} &\Delta F(\Delta L, \Delta d, \Delta T, \Delta P) = \alpha_0 + \alpha_1\Delta L + \alpha_2\Delta d + \alpha_3\Delta T + \alpha_4\Delta P + \alpha_5\Delta L\Delta d \\ &+\alpha_6\Delta L\Delta T + \alpha_7\Delta L\Delta P + a_8\Delta d\Delta T + a_9\Delta d\Delta P + a_{10}\Delta T\Delta P + a_{11}\Delta L^2 \\ &+a_{12}\Delta d^2 + a_{13}\Delta T^2 + a_{14}\Delta P^2 \end{aligned} \tag{10}$$

In order to effectively obtain the 15 constants a_i (i = 0~14) in Eq. (10), orthogonal design can be adopted to work out ΔL, Δd, ΔT and ΔP in the four-variable and five-level orthogonal array (Table 1). And the column values of pure water flux sensitivity ΔF pertaining to 25 groups of increments in Table 1 can be respectively calculated via the fiber operation differential equation (Eq. (6)).

Put the values in each of the five columns of Table 1 into Eq. (10), and each constant a_i (i = 0~14) in Table 2 can be worked out via numerical fitting method. In this context, the polynomial of power functions in Eq. (10) is the function between pure water flux sensitivity and parameter increments.

6. Pure water flux index and flux distribution

Under the standard testing conditions, the along-path flux and water-product flow rate in the "specific membrane fiber" ($\sum\Delta$ = 0) can be calculated using Eq. (6), as shown in Fig. 3. The water-product flow rate Q is 1.305L/h, the fiber surface area $S$is 0.00377 m^2, and the pure water flux $F_{\sum\Delta=0}$ is 346.2L MH. It indicates that the water-product flow rate is zero at the end of the fiber, when under dead operation mode. Velocity of pressure drop is the fastest at the head of the fiber, and the velocity is slow down through the distance. As the flux is almost proportional to the pressure, the distribution curve of the flux along the membrane is similar to that of the pressure.

Fig. 4 shows the corresponding flux distribution along the fiber-path with the change of the four parameters ($\sum\Delta$, ΔT, ΔP and Δd). Compared with "the specific flux" ($\sum\Delta$ = 0), the flux distribution curve is higher and the pure water flux is larger ($F\,\Delta_{T=6}$ = 365.0 LMH), when ΔT is 6°C, due to the characteristics of low temperature membrane. When ΔP is –10 kPa, the flux distribution curve is lower and the pure water flux is smaller ($F\,\Delta_{P=-10\text{kPa}}$ = 341.1 LMH), due to the high pressure membrane characteristics. When Δd is 10 mm, the slope of the flux distribution curve is smaller, and the pure water flux is slightly larger ($F\Delta_{d=10\text{mm}}$ = 349.5 LMH), because of the thicker fiber diameter and the lower resis-

Table 1
Orthogonal table of four variables at five levels about pour water flux of the hollow UF fiber

No.	Fiber length ΔL(m)	Inner diameter Δd (mm)	Temp. ΔT (°C)	Pressure ΔP (kPa)	Average flux F (LMH)*
1	–0.5	–0.10	–6	-10	291
2	–0.5	–0.05	–3	-5	330
3	–0.5	0.00	0	0	356
4	–0.5	+0.05	+3	+5	373
5	–0.5	+0.10	+6	+10	382
6	–0.25	–0.10	–3	0	323
7	–0.25	–0.05	0	+5	352
8	–0.25	0.00	+3	+10	372
9	–0.25	+0.05	+6	–10	365
10	–0.25	+0.10	–6	–5	295
11	0.00	–0.10	0	+10	343
12	0.00	–0.05	+3	–0	361
13	0.00	0.00	+6	–5	362
14	0.00	+0.05	–6	0	292
15	0.00	+0.10	–3	+5	329
16	+0.25	–0.10	+3	–5	342
17	+0.25	–0.05	+6	0	352
18	+0.25	0.00	–6	+5	286
19	+0.25	+0.05	–3	+10	322
20	+0.25	+0.10	0	–10	339
21	+0.5	–0.10	+6	+5	342
22	+0.5	–0.05	–6	+10	277
23	+0.5	0.00	–3	–10	305
24	+0.5	+0.05	0	–5	332
25	+0.5	+0.10	+3	0	350

*: "LMH" means L/(m²·h).
Note: The reference conditions in the Table 1 are: L = 1.5 m, d = 0.8 mm, T = 25°C, P = 100 kPa, that is to say, ΔT = 0, ΔP = 0, ΔT = 0, ΔP = 0 respectively means the condition of L = 1.5 m, d = 0.8 mm, T = 25°C, P = 100kPa.

tance. It can be seen that the influence of the single parameter change on the flux distribution along the fiber and pure water flux.

7. The sensitivity of pure water flux to variation of four parameters

The sensitivity function of pure water flux to variation of four parameters has been shown in the equation above (10), in which, a_1 and a_{11}, a_2 and a_{12}, a_3 and a_{13}, a_4 and a_{14} represent respectively the sensitivity of pure water flux to each of the four changes. Figs. 5–8 show respectively the sensitivity curve between pure water flux and each of the four changes (ΔL, Δd, ΔT and ΔP), in which the cardinal number of pure water flux F = 313.2 LMH.

Table 2
Numerical simulated solutions of the various constants in formula (10) using the data in Table 1

a_0	348.017
a_1	–24.587
a_2	49.556
a_3	6.119
a_4	0.394
a_5	18.018
a_6	0.000
a_7	0.000
a_8	0.778
a_9	1.557
a_{10}	0.005
a_{11}	–13.421
a_{12}	–281.116
a_{13}	–0.565
a_{14}	0.012

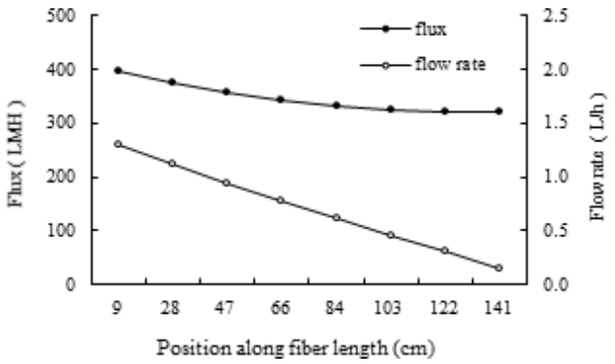

Fig. 3. Parameter distribution under standard testing conditions.

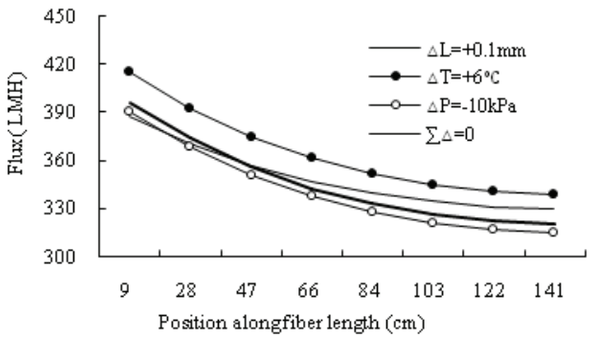

Fig. 4. Flux along the fiber corresponding to each parameter change.

The sensitivity curve of pure water flux and fiber length change, as is shown in Fig. 5, shows that the longer the fiber length is, the greater the water yield is, and the greater pressure drop inside the fiber, the lower pressure difference between the inside and outside of the fiber. Therefore, the

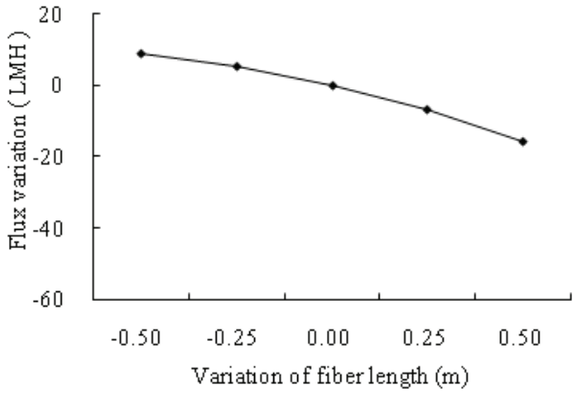

Fig. 5. Sensitivity curve of pure water flux change and fiber length change at the constant operating pressure of 100 kPa, fiber inner diameter of 0.8 mm and temperature of 25°C.

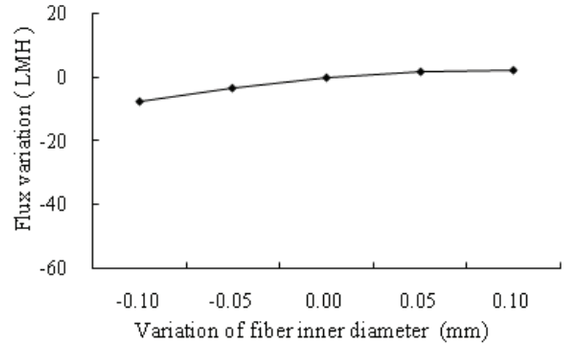

Fig. 6. Sensitivity curve of pure water flux change and fiber inner diameter change at the constant operating pressure of 100 kPa, fiber length of 1.5 m and temperature of 25°C.

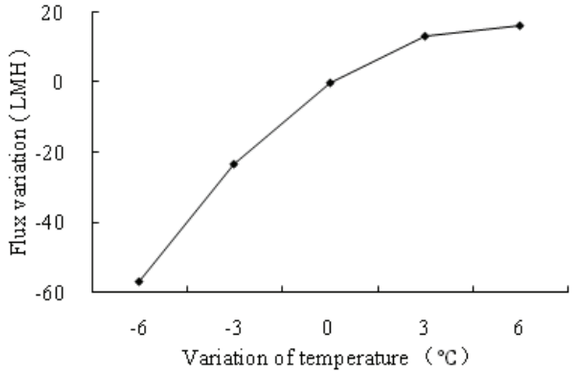

Fig. 7. Sensitivity curve of pure water flux change and temperature change at the constant operating pressure of 100 kPa, fiber inner diameter of 0.8 mm and fiber length of 1.5 m.

average flux of the fiber is lower. As the fiber length changes from –0.5 m to +0.5 m, every increase of 0.1 m leads to pure water flux decreased by 2.46 LMH.

The sensitivity curve of pure water flux to fiber inner diameter change in Fig. 6 indicates that the bigger the inner diameter is, the smaller the resistance of the fiber is, and the smaller pressure drop inside the fiber is, the higher the internal and external pressure difference of the fiber is, the higher the average flux of the fiber is. When the fiber inner diameter increases from –0.1 mm to +0.1 mm, the pure water flux increases by 0.50 LMH for each 0.1 mm increase.

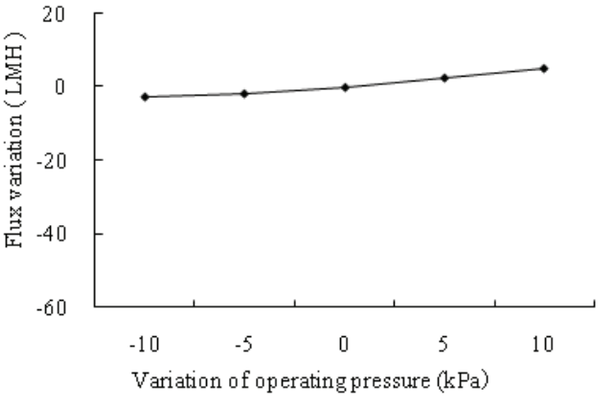

Fig. 8. Sensitivity curve of pure water flux change and pressure change at the constant operating temperature of 25°C, fiber inner diameter of 0.8 mm and fiber length of 1.5 m.

The sensitivity curve of the pure water flux and the temperature change is shown in Fig. 7. It is indicated that the pure water flux of "high-temperature membrane fibers" with a negative T is relatively lower under standard temperature conditions, while it is relatively higher with a positive T. If the temperature increases form –6°C to 0°C, every increase of 1°C could lead to an increase of 9.51 LMH in pure water flux. While if the temperature increases form 0°C to 6°C, every increase of 1°C could only lead to an increase of 2.73 LMH. With the increase of temperature increment from negative to positive, the rising rate of pure water flux will gradually slow down under standard test conditions.

The sensitivity curve of the pure water flux and the pressure change is shown in Fig. 8. It shows that the pure water flux of the "high pressure membrane fiber" with negative ΔP is slightly lower under the standard temperature condition, while the pure water flux of the "low pressure membrane filament" under standard test conditions is slightly higher than the pure water flux. If the pressure increases form –10 kPa to 10 kPa, every increase of 1 kPa could lead to an increase of 0.40 LMH in pure water flux.

8. Conclusions

Through the analysis above, the following conclusions can be drawn for the pure water flux of inside-out hollow ultra filtration membrane fibers under standard testing conditions:

(1) Using the mathematical model of the differential equation, the pure water flux indexes of inside-out membrane fibers, whether under standard testing conditions or conditions of various related parameter changes combined, can be worked out.

(2) By way of orthogonal design and numerical fitting, the sensitivity function of pure water flux index to various parameter increments can be obtained, thus completing the sensitivity analysis of the relation between the pure water flux index and each of the parameter increments. The sensitivity analysis results show that the longer the film length is, the lower the average flux is; the bigger the wire diameter is, the higher the average flux is; the higher the temperature is, the greater the average flux is; the higher the pressure is, the greater the average flux is.
(3) Based on the analysis of the sensitivity of the pure water flux to each of the parameter changes, the influence on pure water flux of changes in a certain specification or property of membrane fibers can be effectively reflected or predicted, and the material formulation or fabrication technique of membrane fibers can be effectively optimized.

In one word, the pure water flux under standard transmembrane pressure difference is a simple and effective index reflecting the overall performance of membrane fibers, but it cannot indicate the respective effects of each important factor inside the fiber, while the responsively analysis of pure water flux and its related parameters is able to reflect the quantitative relationship between different parameters-fiber length, fiber diameter, temperature and pressure-and pure water flux index.

Acknowledgments

This work was financially supported by Stat Key Laboratory of Separation Membranes and Membrane Processes (Tianjin Polytechnic University, China), No. M2-201603) and Key Project of Natural Science Funds of Tianjin, China (No. 15JCZDJC40100).

References

[1] S. Muthukumaran, Performance evaluation of different ultra filtration membranes for the reclamation and reuse of secondary effluent. Desalination, 279 (2011) 383–389.
[2] A. Alturki, J. Mcdonald, S.J Khan, F.I. Hai, W.E. Price, L.D. Nghiem, Performance of a novel osmotic membrane bioreactor (OMBR) system: Flux stability and removal of trace organics, Bioresour. Technol., 113 (2012) 201–210.
[3] Praveen, Nguyen, Loh, Biodegradation of phenol from saline wastewater using forward osmotic hollow fiber membrane bioreactor coupled chemostat, Biochem. Eng. J., 94 (2015) 125–133.
[4] G.B. Li, H. Liang, Zero irreversible flux for ultra filtration and its application in water treatment process, J. China Water Wastewater, 28 (2012) 5–7.
[5] J.X. Li, X.H. Li, H. Wang, B.Q. He, J. Wang, H.W. Zhang, J.J. Li, Mathematical modeling for the local flux distribution of submerged hollow fiber membrane module, Membr. Sci. Technol., 35 (2015) 1–5.
[6] X.H. Li, J.X. Li, J. Wang, H. Wang, Experimental investigation of local flux distribution and fouling behavior in double-end and dead-end submerged hollow fiber membrane modules, J. Membr. Sci., 453 (2014) 18–26.
[7] X.H. Li, J.X. Li, H. Wang, A filtration model for prediction of local flux distribution and optimization of submerged hollow fiber membrane module, AIChE J., 61 (2015) 4377–4386.
[8] L.W. Zhuang, G.C. Dai, Numerical simulation of dynamic process during outside-in dead-end filtration in hollow fiber membrane module, J. CIESC, 67 (2016) 2841–2850.
[9] L.W. Zhuang, G. Dai, Numerical simulation of flux distribution in the hollow fiber ultra filtration membrane module, Membr. Sci. Technol., 36 (2016) 86–95.
[10] C. Liu, X.L Lv, C.R. Wu, X. Wang, Q.J. Gao, H.Y. Chen, Y. Jia, Discussing about critical operating flux of ultra filtration membrane, Membr. Sci. Technol., 37 (2017) 23–26.
[11] Y.P. Zhang, X.L. Wang, J. Liu, Y.H. Wang, X.H. Pan, J. Hao, Evaluation of uncertainty in measurement of pure water flux of hollow fiber ultra filtration membrane, Technol. Water Treat., 40 (2014) 53–56.
[12] J. Gunther, P. Schmitz, C. Albasi, C. Lafforgue, A numerical approach to study the impact of packing density on fluid flow distribution in hollow fiber module, J. Membr. Sci., 348 (2010) 277–286.
[13] Y.S Polyakov, Dead-end outside in hollow-fiber membrane filter: Mathematical model, J. Membr. Sci., 279 (2006) 615–624.
[14] S. Lin, Effect of operating parameters on the separation of proteins in aqueous solutions by dead-end ultra filtration, Desalination, 234 (2008) 116–125.
[15] A.K. Pavanasam, A. Abbas, V. Chen, Influence of particle size and operating parameters on virus ultra filtration efficiency, Water Sci. Technol. Water Supply, 11 (2011) 31–38.
[16] E. Alventosa-Delara, S. Barredo-Damas, M. Alcaina-Miranda, M.I. Iborra-Clar, Ultra filtration technology with a ceramic membrane for reactive dye removal: optimization of membrane performance, J. Hazard. Mater., 209 (2012) 492–500.
[17] S.H. Yoon, S.H. Lee, I.T. Yeom, Experimental verification of pressure drop models in hollow fiber membrane, J. Membr. Sci., 310 (2008) 7–12.
[18] K.B. Lim, et al., Computational studies for the design parameters of hollow fibre membrane modules, J. Membr. Sci., 529 (2017) 263–273.
[19] M. Mehdipourghazi, S. Barati, F. Varaminian, Mathematical modeling and simulation of carbon dioxide stripping from water using hollow fiber membrane contactors, Chem. Eng. Process.: Process Intens., 95 (2015) 159–164.
[20] S. Chang, A.G Fane, The effect of fibre diameter on filtration and flux distribution-relevance to submerged hollow fibre modules, J. Membr. Sci., 184 (2001) 221–231.
[21] Z.C. Zhang, H.Y. Yuan, Pure water flux distribution in form of single-ended and double-ended water supply of the internal pressure-type ultra filtration membrane fiber, Ind. Water Treat., 36 (2016) 70–73.